PHYSICAL REVIEW B **91**, 201108(R) (2015)

Absence of orbital rotation in superconducting $CeCu_2Ge_2$

J.-P. Rueff,[1,2,*] J. M. Ablett,[1] F. Strigari,[3] M. Deppe,[4] M. W. Haverkort,[4] L. H. Tjeng,[4] and A. Severing[3]

[1]*Synchrotron SOLEIL, L'Orme des Merisiers, Saint-Aubin, Boîte Postale 48, 91192 Gif-sur-Yvette Cedex, France*

[2]*Laboratoire de Chimie Physique–Matière et Rayonnement, CNRS-UMR 7614, Université Pierre et Marie Curie, F-75005 Paris, France*

[3]*Institute of Physics II, University of Cologne, Zülpicher Straße 77, D-50937 Cologne, Germany*

[4]*Max Planck Institute for Chemical Physics of Solids, Nöthnizer Straße 40, D-01187 Dresden, Germany*

(Received 7 November 2014; revised manuscript received 30 April 2015; published 26 May 2015)

We address the recently proposed orbital transition scenario in heavy fermion compounds exhibiting two superconducting domes. Our method of choice is nonresonant inelastic x-ray scattering (NIXS) which probes charge densities and can be modeled quantitatively. Our NIXS results of $CeCu_2Ge_2$, a model system of this class of materials, are well described by considering the same sequence of orbitals at all temperatures, thus putting into question whether orbital transitions are related to the formation of the second superconducting dome. The discrepancy between experimental findings and prediction could be due to the lack of accuracy in the theoretical description of the $4f$ states.

DOI: 10.1103/PhysRevB.91.201108 PACS number(s): 71.27.+a, 71.20.Eh, 74.25.Jb, 78.70.Ck

Rare-earth-based ($4f$) heavy fermion (HF) compounds have attracted considerable interest over the past decade because they realize most of the exotic phenomena in condensed matter physics such as non-Fermi-liquid behavior [1], unconventional superconductivity (SC) [2,3], quantum criticality [4], or a topological insulating state [5]. $CeCu_2Si_2$ especially has been extensively studied being considered as the seminal system for unconventional HF superconductivity [6]. At low temperatures, $CeCu_2Si_2$ and also the related compound $CeCu_2Ge_2$ exhibit a two-dome superconducting phase when pressure is applied. This "potato shape" phase was later confirmed in a vast class of materials [7] including $CeNi_2Ge_2$, $CeCoIn_5$, $CeIrIn_5$, $CePt_3Si$, or $CeIrSi_3$ making it a characteristic feature of $4f$ unconventional superconductivity. As it turns out, the two-dome superconducting state is even more widely spread than the single-dome phase, which makes its understanding even more stringent. The low pressure superconducting dome (SC-I) emerges next to the antiferromagnetic (AFM) phase (see phase diagram in Fig. 1) [8] and it is generally accepted that spin fluctuations trigger the formation of this superconducting state. However, in spite of extensive work, the reemergence of superconductivity at high pressure (SC-II phase) remains conceptually challenging. The remoteness of the SC-II phase from the AFM phase makes it unlikely that the superconductivity is driven by the spin fluctuation. Instead, a valence critical fluctuation (VCF) model was proposed by Onishi and Miyake [9] where the onset of the SC-II phase should go along with sizable and abrupt fluctuations of the number of f electrons n_f in the presence of a strong on-site Coulomb repulsion U. Previous studies of $CeCu_2Si_2$ [10] and $CeCu_2Ge_2$ [11] tested the VCF model with high-resolution, lifetime removed, x-ray absorption spectroscopy at the Ce L_3 edge under pressure and at low temperatures. In both systems a decrease of n_f close to the SC-II dome was found, but the small amplitude of the variation ($\sim$10%) and the smooth character of the valence decay does not convincingly argue for the VCF model.

In more recent studies based on a dynamical mean-field theory (DMFT) approach, Hattori [15] and Pourovskii *et al.* [14] have independently underlined the role of orbital fluctuations as a key ingredient for understanding the onset of the SC-II phase. Both models imply a "metaorbital" transition between two crystalline electric field (CEF) states with different hybridizations. Recently, Ren *et al.* [16] also pointed out the importance of orbital physics for the formation of superconductivity in pressurized $CeAu_2Si_2$. In this work, we will more specifically discuss the results of Pourovskii *et al.* [14] as the authors made clear predictions for where to look in the phase diagram in order to observe orbital fluctuations. Furthermore, they calculated spectral signatures of the orbital transition in the nonresonant inelastic x-ray scattering (NIXS) cross section that can be directly compared to our experimental results.

We recall that a tetragonal CEF splits the sixfold degenerate Hund's rule ground state of Ce^{3+} into three Kramers doublets of type $\Gamma_7^1 = \alpha\,|\pm 5/2\rangle + \sqrt{1-\alpha^2}\,|\mp 3/2\rangle$, $\Gamma_7^2 = \sqrt{1-\alpha^2}\,|\pm 5/2\rangle - \alpha\,|\mp 3/2\rangle$, and $\Gamma_6 = |\pm 1/2\rangle$. Here the J_z representation has been chosen with α as the occupation ratio of the respective $|5/2\rangle$ and $|3/2\rangle$ J_z states. The two states Γ_7^1 and Γ_7^2 differ in their J_z admixture and in their sign of α, i.e., they are Π-type orbitals ($++$ or $--$) with their lobes along [100] or Σ-type orbitals ($+-$ or $-+$) with lobes along the [110] direction. It is important to recognize that Π- and Σ-type orbitals are rotated to one another by 45° [see Fig. 1(a)].

Goremychkin *et al.* investigated the CEF scheme of $CeCu_2Si_2$ with inelastic neutron scattering and found a Γ_7 ground state and two pseudodegenerate excited states at about 30 meV, i.e., $\Delta E_1 \approx \Delta E_2$ [see top panel of Fig. 1(a)] [12]. However, determining the sign of α was only recently achieved with a NIXS experiment by Willers *et al.* [13]. It turns out that α in $CeCu_2Si_2$ is negative at ambient pressure and $T \ll \Delta E_{1,2}$, so that using our nomenclature, a Σ-type Γ_7 state with lobes pointing along the [110] direction forms the ground state [see projection in Fig. 1(a)]. In the following discussion, we will refer to Π- and Σ-type states in order to avoid confusion.

How does this match the predictions of the orbital transition scenario? The DMFT calculations suggest, at zero pressure [p_{c1} in Fig. 1(b)] and low T conditions, a Π-type Γ_7 ground

*Corresponding author: jean-pascal.rueff@synchrotron-soleil.fr

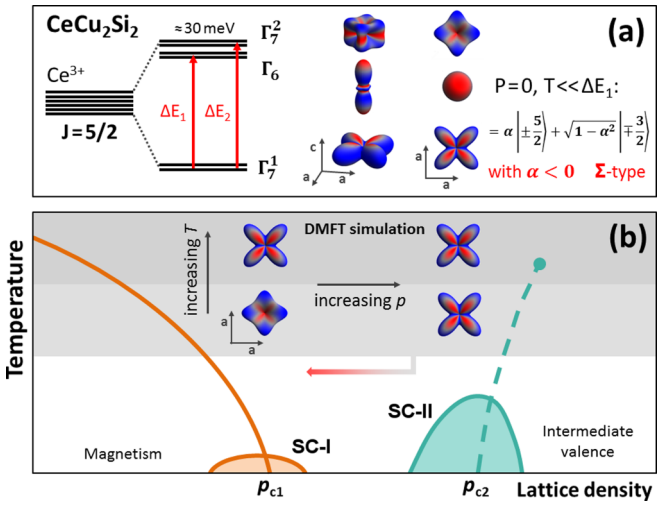

FIG. 1. (Color online) (a) Crystal-field split Hund's rule ground state in tetragonal point symmetry of Ce^{3+}. The energy splittings and order of states are as measured in $CeCu_2Si_2$, i.e., with a Σ-type ground state ($\alpha < 0$) [12,13]. (b) Schematic phase diagram of Ce-based narrow-band metals as adapted from [8]. The orientation of the orbital plots refers to the DMFT calculations by Pourovskii *et al.* [14]. The red arrow illustrates the pressure shift necessary to match the experimental and theoretical ground states (see text for details).

state orbital (referred to as state $|0\rangle$ in Ref. [14]) with lobes pointing along [100]. The occupation of the Σ-type Γ_7 state (state $|2\rangle$ in Ref. [14]) is predicted to increase with either temperature or pressure and eventually become dominant at high pressure, i.e., in the strong-coupling regime [see p_{c2} in Fig. 1(b)]. As it turns out, however, early experimental results have established that the Σ-type state is already the ground state at ambient pressure and 20 K [compare Figs. 1(a) and 1(b)] [13]. Moreover, there are no indications for an orbital flipping at even lower temperatures or with rising temperature according to inelastic neutron scattering and static susceptibility measurements [12]. This apparent contradiction does not necessarily disqualify the metaorbital transition scenario provided the theoretical pressure (and/or hybridization) axis is shifted by several GPa such that $CeCu_2Si_2$ at ambient pressure and low T already corresponds to the strongly hybridized region in the calculation [see red arrow in Fig. 1(b)]. As a direct consequence of such a rescaling, a different orbital orientation is predicted at negative pressures or in materials with less hybridization. In particular, we expect a reversal of the Π- and Σ-type states as a function of temperature (besides the mere changes due to thermal occupation of excited CEF states) as illustrated in Fig. 1(b), and consequently a flipping of the Ce $N_{4,5}$ NIXS dichroic spectra [Fig. 3(b)] as explained below.

In this work, we have chosen to test the above conjecture in $CeCu_2Ge_2$. This Ge compound behaves like $CeCu_2Si_2$ at a negative pressure (of about -12 GPa) due to the larger Ge ionic radius [8] and therefore appears as an ideal candidate for our study. As pointed out above, the fundamental difference between the two Γ_7 states is the altered orbital orientation with respect to the unit-cell axis, but unfortunately none of the commonly used techniques such as inelastic neutron scattering or x-ray absorption are sensitive to anisotropies with a higher than twofold rotational axis. Here NIXS is more powerful because the transition operator $\exp(i\mathbf{q}\cdot\mathbf{r})$ that enters the scattering function may lead to nondipolar transition operators depending on the amplitude of the momentum transfer $|\mathbf{q}|$. When $|\mathbf{q}| \gg 1$ the exponential can no longer be limited to the first order (dipole). For large $|\mathbf{q}|$ higher rank operators have to be considered. Calculations of the scattering function have confirmed that the $N_{4,5}$ NIXS spectra of rare earths at $|\mathbf{q}| \sim 10$ Å are dominated by third (octupole) and fifth (triakontadipole) order contributions [17–24], thus enabling us to probe anisotropies with fourfold rotational symmetry as later demonstrated in the work of Ref. [13]. More precisely, the NIXS $N_{4,5}$ edges were shown to exhibit a clear dichroism $I_{100} - I_{110}$ when measuring the scattering intensity I with $\mathbf{q}\|[100]$ and $\mathbf{q}\|[110]$. The sign of the dichroic signal allows the distinction between the Π- and Σ-type ground states. Our expectations when using $CeCu_2Ge_2$ as representative for the low coupling regime is twofold: First, to establish the signature of the Π-type state in the NIXS dichroic spectrum at low temperature ($T \lesssim 20$ K)—the expected spectrum is to be opposite to that of $CeCu_2Si_2$ [13]; second, to monitor a flipping of the dichroic signal as temperature is increased in agreement with the orbital transition scenario which predicts a dominating Σ-type state at high temperatures [see Fig. 1(b)].

The samples were cut from a single crystal grown by the Czochralski method in a tri-arc furnace using a $CeCu_2Ge_2$ ingot prepared from the pure elements. The crystal orientation was determined by Laue technique. The experiment was carried out at the GALAXIES beamline at the SOLEIL synchrotron [25], using the beamline NIXS multianalyzer spectrometer. The spectrometer consists of a set of four Si(660) 1 m radius spherically bent crystal analyzers arranged in 2×2 array so as to augment the solid angle. The analyzers were operated at a fixed Bragg angle of 86° at 9721 eV in the Rowland circle geometry. The total beamline and spectrometer resolution was estimated to be about 1.25 eV by measuring the elastic line of a thin Scotch tape. Two crystals were cut prior to the measurements with either the [100] or [110] direction normal to the surface. For low temperature measurements the samples were mounted in a He-cooled cryostat and properly aligned with their surface normal parallel to the momentum transfer direction $\mathbf{q}$. We used an avalanche photodiode as detector. To enhance the nondipolar contribution form the NIXS cross section, the measurements were performed at a scattering angle of 150° corresponding to a momentum transfer $|\mathbf{q}| = 9.5\,\text{Å}^{-1}$ which is well within the nondipolar regime.

Figure 2 shows the NIXS intensity as a function of the energy transfer ΔE for $CeCu_2Ge_2$ at low (~7 K) and room temperature for both sample orientations. The total counting time for each spectrum was about 12 h. For reasons of comparison, the spectra were normalized to the total area. At 7 K the Ce $N_{4,5}$ NIXS spectra of $CeCu_2Ge_2$ exhibit a sizable dichroic signal which is similar to the simulations (cf. Fig. 3) and to the previously reported measurements of $CeCu_2Si_2$. With rising temperature the dichroic effect decreases without changing sign. According to the phase diagram of Fig. 1, we

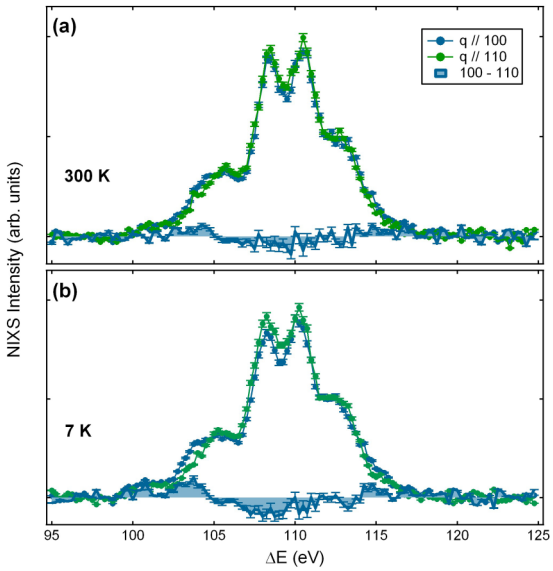

FIG. 2. (Color online) Experimental Ce $N_{4,5}$ NIXS spectra in $CeCu_2Ge_2$ at 300 K (a) and 7 K (b). The NIXS spectra were measured with $\mathbf{q} \parallel [100]$ and $\mathbf{q} \parallel [110]$. The resulting dichroic spectra $I_{100} - I_{110}$ are displayed below the NIXS spectra as filled curves.

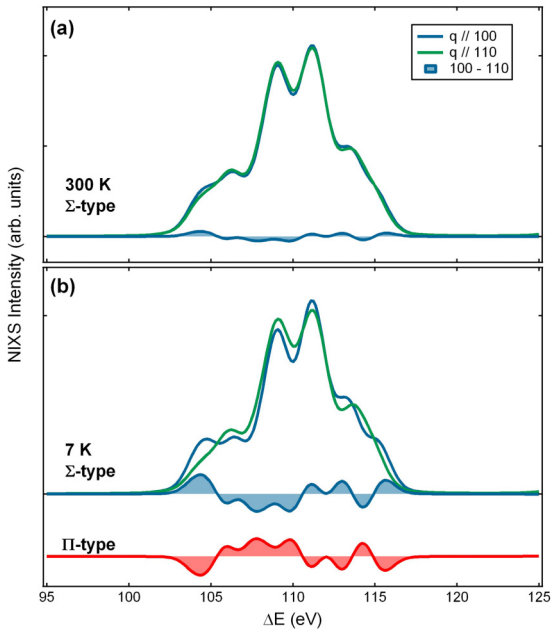

FIG. 3. (Color online) Calculated Ce $N_{4,5}$ NIXS spectra for 9.3 Å at 300 K (a) and 7 K (b) for two $\mathbf{q}$ directions on the basis of an Σ-type ground state and crystal-field splittings as described in Fig. 1. The filled curves represent the difference in intensity, $I_{100} - I_{110}$ for the Σ-type ground state, and the Π-type ground state at 7 K.

should see a transition of the orbital ground state—thus a sign change of the dichroic signal—when passing from the low temperature to the high temperature region in $CeCu_2Ge_2$ and, additionally, when comparing $CeCu_2Ge_2$ at low temperature and $CeCu_2Si_2$ at 20 K. None of these are observed here.

The theoretical spectra are depicted in Fig. 3. The Ce $N_{4,5}$ NIXS edges were simulated at $|\mathbf{q}| = 9.3$ Å^{-1} in the nondipolar regime for $\mathbf{q}$ parallel to both the [100] and [110] directions at 7 K (bottom) and 300 K (top). For the simulations we used the code of Ref. [26]; a more detailed description for this specific application of the code can be found in Ref. [13]. The two panels in Fig. 3 show the simulated NIXS spectra on the basis of a Σ-type Γ_7^1 ground state *à la* $CeCu_2Si_2$ at all temperatures. For the simulations we used the wave function and energy splittings $\Delta E_1 = 17$ meV and $\Delta E_2 = 18.3$ meV as obtained from neutron data [27,28]. At 7 K a clear dichroic signal $I_{100} - I_{110}$ is visible and its spectral line shape agrees well with the experimental data. We therefore conclude the Si and Ge compounds have the same Σ-type Γ_7 ground state. The simulations show further that the dichroic signal should be inversed when a Π-type ground state is considered [see Fig. 3(b), bottom]. For the 300 K simulation the thermal occupation of the excited states has been taken into account, i.e., 52% of Γ_7^1 and 24% and 26% for Γ_7^2 and Γ_6. The pure J_z state Γ_6 has been included, although it does not contribute to the dichroic signal due to its rotational symmetry [see Fig. 1(a)]. The temperature change of the dichroic signal is well explained by the thermal population of excited CEF states [29]. Overall, the simulations reveal the Σ-type character of the $CeCu_2Ge_2$ ground state at all temperatures.

Without excluding gradual changes of the CEF wave functions as a function of hybridization or temperature, we do exclude changes in the order of CEF states due to increasing hybridization or temperature from the present data on $CeCu_2Ge_2$ and the information available on $CeCu_2Si_2$. We find the Σ-type Γ_7 state to be the ground state under all conditions, i.e., for stronger ($CeCu_2Si_2$) and weaker hybridization ($CeCu_2Ge_2$) at low and at high temperatures. Nevertheless, the idea by Hattori [15] that different f orbitals hybridize differently with the conduction band, thus leading to different energy gains, might still be valid. The experimental results only state that possibly occurring *orbital transitions* do not occur in the phase diagram where Pourovskii *et al.* had predicted. This discrepancy between experiment and theoretical LDA+DMFT predictions for the orbital occupation might be due to issues in the double counting corrections of the nonspherical part of the local Coulomb repulsion [30,31]. In order to describe rare-earth materials from first principles an accuracy of the $4f$ crystal field levels better than 10 meV is needed, which currently is challenging. A possible solution could be the calculation of the nonspherical DFT potential that arises due to the occupied f orbitals and the subtraction of this potential from the DFT potential, which is then replaced by the full many-body interaction in a DMFT loop. Another option could be to treat the local DFT potential on the f shell in spherical symmetry, either by using warped potentials [26] or by placing the f orbitals in the core when the DFT potential is calculated [32–34].

In conclusion, our results demonstrate the absence of an orbital transition in $CeCu_2Ge_2$ as a function of temperature and also with respect to $CeCu_2Si_2$ which is considerably stronger hybridized. Such an orbital transition would have manifested itself in a change of orbital orientation which again would have given rise to a reversed dichroism in the Ce $N_{4,5}$ NIXS spectra which were measured beyond the dipole limit. Such a change of dichroism has not been observed. While the orbital

transition scenario is likely not related to the formation of the second superconducting dome or does not occur in the phase diagram where predicted, our results do not exclude the possibility of an orbital-dependent hybridization of the f electrons with the conduction band and call for more accurate theoretical treatments of the f states.

We are grateful to L. Pourovskii, Ph. Hansmann, and A. Georges for their insights about the orbital transition scenario. We acknowledge D. Jaccard, C. Geibel, and P. Thalmeier for fruitful discussions. For F.S. and A.S this work was supported by the German Funding Agency (DFG) through Project No. 600575. The experimental work was performed on the GALAXIES beamline using the high-pressure support laboratory at the SOLEIL Synchrotron, France (Proposal No. 99130192). We are grateful to the SOLEIL staff for their assistance and for smoothly running the facility.

[1] H. v. Löhneysen, A. Rosch, M. Vojta, and P. Wölfle, Rev. Mod. Phys. **79**, 1015 (2007).

[2] P. Thalmeier and G. Zwicknagl, *Unconventional Superconductivity and Magnetism in Lanthanide and Actinide Intermetallic Compounds*, Handbook on the Physics and Chemistry of Rare Earths Vol. 34 (Elsevier, New York, 2004), pp. 135–287.

[3] B. B. Zhou, S. Misra, E. H. da Silva Neto, P. Aynajian, R. E. Baumbach, J. D. Thompson, E. D. Bauer, and A. Yazdani, Nat. Phys. **9**, 474 (2013).

[4] Q. Si and F. Steglich, Science **329**, 1161 (2010).

[5] M. Dzero, K. Sun, V. Galitski, and P. Coleman, Phys. Rev. Lett. **104**, 106408 (2010).

[6] F. Steglich, J. Aarts, C. D. Bredl, W. Lieke, D. Meschede, W. Franz, and H. Schäfer, Phys. Rev. Lett. **43**, 1892 (1979).

[7] A. T. Holmes, D. Jaccard, and K. Miyake, J. Phys. Soc. Jpn. **76**, 051002 (2007).

[8] H. Q. Yuan, F. M. Grosche, M. Deppe, C. Geibel, G. Sparn, and F. Steglich, Science **302**, 2104 (2003).

[9] Y. Onishi and K. Miyake, J. Phys. Soc. Jpn. **69**, 3955 (2000).

[10] J.-P. Rueff, S. Raymond, M. Taguchi, M. Sikora, J.-P. Itié, F. Baudelet, D. Braithwaite, G. Knebel, and D. Jaccard, Phys. Rev. Lett. **106**, 186405 (2011).

[11] H. Yamaoka, Y. Ikeda, I. Jarrige, N. Tsujii, Y. Zekko, Y. Yamamoto, J. Mizuki, J.-F. Lin, N. Hiraoka, H. Ishii, K.-D. Tsuei, T. C. Kobayashi, F. Honda, and Y. Ōnuki, Phys. Rev. Lett. **113**, 086403 (2014).

[12] E. A. Goremychkin and R. Osborn, Phys. Rev. B **47**, 14280 (1993).

[13] T. Willers, F. Strigari, N. Hiraoka, Y. Q. Cai, M. W. Haverkort, K.-D. Tsuei, Y. F. Liao, S. Seiro, C. Geibel, F. Steglich, L. H. Tjeng, and A. Severing, Phys. Rev. Lett. **109**, 046401 (2012).

[14] L. V. Pourovskii, P. Hansmann, M. Ferrero, and A. Georges, Phys. Rev. Lett. **112**, 106407 (2014).

[15] K. Hattori, J. Phys. Soc. Jpn. **79**, 114717 (2010).

[16] Z. Ren, L. V. Pourovskii, G. Giriat, G. Lapertot, A. Georges, and D. Jaccard, Phys. Rev. X **4**, 031055 (2014).

[17] J. A. Soininen, A. L. Ankudinov, and J. J. Rehr, Phys. Rev. B **72**, 045136 (2005).

[18] W. Schülke, *Electron Dynamics by Inelastic X-Ray Scattering* (Oxford University Press, Oxford, 2007).

[19] M. W. Haverkort, A. Tanaka, L. H. Tjeng, and G. A. Sawatzky, Phys. Rev. Lett. **99**, 257401 (2007).

[20] R. A. Gordon, G. T. Seidler, T. T. Fister, M. W. Haverkort, G. A. Sawatzky, A. Tanaka, and T. Sham, Europhys. Lett. **81**, 26004 (2008).

[21] J. A. Bradley, G. T. Seidler, G. Cooper, M. Vos, A. P. Hitchcock, A. P. Sorini, C. Schlimmer, and K. P. Nagle, Phys. Rev. Lett. **105**, 053202 (2010).

[22] R. Caciuffo, G. van der Laan, L. Simonelli, T. Vitova, C. Mazzoli, M. A. Denecke, and G. H. Lander, Phys. Rev. B **81**, 195104 (2010).

[23] J. A. Bradley, K. T. Moore, G. van der Laan, J. P. Bradley, and R. A. Gordon, Phys. Rev. B **84**, 205105 (2011).

[24] G. van der Laan, Phys. Rev. Lett. **108**, 077401 (2012).

[25] J.-P. Rueff, J. M. Ablett, D. Céolin, D. Prieur, T. Moreno, V. Balédent, B. Lassalle, J. E. Rault, M. Simon, and A. Shukla, J. Synchrotron Radiat. **22**, 175 (2015).

[26] M. W. Haverkort, M. Zwierzycki, and O. K. Andersen, Phys. Rev. B **85**, 165113 (2012).

[27] G. Knopp, A. Loidl, K. Knorr, L. Pawlak, M. Duczmal, R. Caspary, U. Gottwick, H. Spille, F. Steglich, and A. Murani, Z. Phys. B **77**, 95 (1989).

[28] M. Loewenhaupt, E. Faulhaber, A. Schneidewind, M. Deppe, and K. Hradil, J. Appl. Phys. **111**, 07E124 (2012).

[29] See Supplemental Material at http://link.aps.org/supplemental/10.1103/PhysRevB.91.201108 for full population temperature dependence of the Γ states.

[30] M. Aichhorn, L. Pourovskii, V. Vildosola, M. Ferrero, O. Parcollet, T. Miyake, A. Georges, and S. Biermann, Phys. Rev. B **80**, 085101 (2009).

[31] If one calculates the LDA potential for a Ce atom with a single electron in the $j_z = 7/2$ orbital, the resulting potential does not have spherical symmetry due to the nonspherical charge distribution. These potentials resemble the nonspherical multiplet interactions between electrons which is included in local-density approximation (LDA) on a mean-field level. As these interactions are also fully included in the local impurity calculated in the DMFT one needs to do a double counting correction. Several schemes are available, whose accuracies still need to be tested against experiment.

[32] P. Novák, K. Knížek, and J. Kuneš, Phys. Rev. B **87**, 205139 (2013).

[33] P. Novák, K. Knížek, M. Maryško, Z. Jirák, and J. Kuneš, J. Phys.: Condens. Matter **25**, 446001 (2013).

[34] P. Novák, V. Nekvasil, and K. Knížek, J. Magn. Magn. Mater. **358**, 228 (2014).